FULL PAPER

Pharmacology

Small extracellular vesicles from rat plasma promote migration and proliferation of vascular smooth muscle cells

Kosuke OTANI[1)], Mai YOKOYA[1)], Yusei FUJIOKA[1)], Muneyoshi OKADA[1)] and Hideyuki YAMAWAKI[1)]*

[1)]Laboratory of Veterinary Pharmacology, School of Veterinary Medicine, Kitasato University, Towada, Aomori 034-8628, Japan

ABSTRACT. Small extracellular vesicles (sEV) contain various molecules and mediate cell-to-cell communication under both physiological and pathological conditions. We have recently reported that sEV isolated from plasma of normotensive Wistar Kyoto rats (WKY) and spontaneously hypertensive rats (SHR) regulate systemic blood pressure. The initiation and development of hypertension partly rely on proliferation and migration of vascular smooth muscle cells (SMCs) followed by the structural remodeling of vascular wall. In the present study, we examined the effects of plasma sEV in WKY and SHR on the proliferative and migratory functions of primary rat aortic SMCs. There was no difference in the concentration and size distribution of plasma sEV between WKY and SHR, while the protein expression of CD81 in plasma sEV from SHR was lower than that from WKY. Both plasma sEV from WKY and SHR were internalized into SMCs and stimulated the migration and proliferation with a similar potency. In summary, we, for the first time, demonstrated that plasma sEV in WKY and SHR are physiologically active in terms of proliferative and migratory functions, however, these effects do not seem to be related to the pathogenesis of hypertension development.

KEY WORDS: hypertension, plasma, small extracellular vesicles, spontaneously hypertensive rat, vascular smooth muscle cell

Small exstracellular vesicles (sEV, also called exosomes), which are a kind of EV, are enclosed by a lipid-bilayer with a diameter of approximately 50–150 nm and exist in a body fluid with a density of 1.13–1.19 g/ml [39, 45]. They are assembled by intruding into late endosomes in cytosol and released into extracellular fluid through the fusion to cellular membranes. Various molecules such as protein, mRNA, microRNA (miR), DNA, and lipid, are packaged in sEV and thus protected from the resolving enzymes [4, 13, 44]. The sEV as molecular cargoes affect cellular function via signal transduction by binding to receptors and/or transferring the loads through endocytosis and membrane fusion. Therefore, it is recently recognized that sEV mediate cell-to-cell communication under both physiological and pathological conditions [16, 24]. For instance, it is well documented that sEV mediate the development of cancer [3, 47], neurodegeneration [11, 17], and immune diseases [38]. The sEV also regulate the progression and/or prevention of cardiovascular diseases, such as myocardial infarction [7, 20], atherosclerosis [25, 48], and pulmonary hypertension [1, 18]. In addition, we have recently reported that sEV isolated from plasma of normotensive Wistar Kyoto rats (WKY) and spontaneously hypertensive rats (SHR), an animal model of human essential hypertension, regulate the systemic blood pressure [28].

The pathological development of hypertension partly relies on the proliferation and migration of vascular smooth muscle cells (SMCs) followed by the structural remodeling of vascular wall [10, 42]. Migration of SMCs from the medial layer into intima region leads to the neointimal thickening of the artery, which is a kind of structural remodeling of vascular wall. Alternatively, proliferation and migration of SMCs within the medial layer also lead to the thickening of the artery, which is another kind of structural remodeling of vascular wall. The migratory effects of sEV derived from the adventitial fibroblasts of SHR and plasma of the patients with coronary artery disease on vascular SMCs were reported [26, 41]. It was also reported that sEV derived from pulmonary arterial endothelial cells stimulated with lipopolysaccharide promoted the proliferation of vascular SMCs [49]. Comprehensive analysis of miR expression in plasma sEV between WKY and SHR indicated the different expression profiles of miR specifically regulating transforming growth factor-β and mitogen-activated protein kinase pathways, which are related to cellular function [21]. However, the effects of plasma sEV from WKY and SHR on the proliferation and migration of vascular SMCs remain unknown. In the present study, we aimed to clarify them.

MATERIALS AND METHODS

Animals

All animal care and procedures were conducted in conformity with the institutional guideline of School of Veterinary Medicine, the Kitasato University. The animal study was approved by the ethical committee of School of Veterinary Medicine, the Kitasato University. Male Wistar Kyoto rats (WKY), spontaneously hypertensive rats (SHR, Hoshino Laboratory Animals, Inc., Ibaraki, Japan), and normal Wistar rats (CLEA Japan, Inc., Tokyo, Japan) were introduced. The rats can freely take food (CE2, CLEA Japan) and tap water.

sEV isolation from plasma

sEV were isolated from plasma of WKY (WsEV) and SHR (SsEV) by the precipitation with polyethylene-glycol and ultracentrifugation [27]. WKY and SHR (6-week-old) were deeply anesthetized with urethane (Sigma-Aldrich, St. Louis, MO, USA) (1.5 g/kg, i.p.), and blood was drawn via an inferior vena cava. The collected blood samples were gently mixed with heparin at a final concentration of 1 U/ml and centrifuged (1,000 × g, room temperature: RT, 10 min) by using a microcentrifuge (model 3740, Kubota Corp., Tokyo, Japan) to separate plasma. The plasma samples were centrifuged (10,000 × g, 4°C, 10 min), and the supernatant was mixed with an equal volume of sterilized polyethylene-glycol solution consisting of 16% polyethylene-glycol (MW=6,000, FUJIFILM Wako Pure Chemical, Osaka, Japan) and 1 M NaCl (Nacalai Tesque, Kyoto, Japan) by inverting (4°C, overnight). After centrifugation (2,500 × g, 4°C, 15 min), the supernatants were discarded. The pellets were resuspended in sterilized phosphate-buffered saline (PBS) by vigorous vortex (RT, 30 min) and ultracentrifuged (164,071 × g, 4°C, 35 min) by using an Optima XL-80K ultracentrifuge with a swing rotor SW 55 Ti (Beckman Coulter Inc., Miami, FL, USA). The pellets were resuspended in sterilized PBS, which were used for the following examinations.

Concentration and size distribution of plasma sEV

The concentration and size distribution of the isolated vesicles were measured by a tunable resistive pulse sensing (TRPS) method using a qNANO instruments with an NP150 nanopore at 46.0–47.0 mm stretch (IZON Science, Christchurch, New Zealand), which was coated with a TRPS Reagent Kit (IZON Science) for the prevention of sEV adhesion according to a manufacturer's instruction [27]. Raw data were standardized by carboxylated-polystyrene particles with a known diameter of 110 nm.

Protein expression in plasma sEV

The protein expression in plasma sEV was determined by Western blotting as previously described [27]. Protein lysates of sEV were extracted using a radio-immunoprecipitation assay buffer containing 20 mM Tris-HCl (pH7.5), 150 mM NaCl, 10 mM $MgCl_2$, 1% Triton-X, 0.5% sodium deoxycholate, 0.1% sodium dodecyl sulfate, 1% protease inhibitor mixture, and 1% phosphatase inhibitor mixture (Nacalai Tesque) (4°C, 10 min). Protein concentration was measured by using a Pierce BCA protein assay kit (Pierce, Rockford, IL, USA). After equal amounts of protein were separated by SDS-PAGE (7.5 and 14%, 80–120 V, 1.5 hr), they were transferred to a nitrocellulose membrane (Pall Corporation, Ann Arbor, MI, USA) (400 mA, 1.5 hr). To confirm the equal loading of protein, the membranes were stained with 0.1% Ponceau-S/5% acetic acid solution. The Ponceau-S stained membranes were scanned in visible light by using the ATTO light capture system (ATTO, Tokyo, Japan). The total density of all the visible bands in each lane was measured as the amount of total protein using CS analyzer 3.0 software (ATTO). After being blocked with 0.5% skim milk in Tris-buffered saline (TBS) with 0.1% tween 20 (TBS-T), the membranes were incubated with a primary antibody (1:500 dilution in TBS-T, 4°C, overnight). They were detected by using an HRP-conjugated secondary antibody (1:10000 dilution in TBS-T, RT, 1 hr) and the EZ-ECL reagent (Biological Industries, Kibbutz Beit Hesmek, Israel). The results were analyzed using CS analyzer 3.0 software. The antibody sources for Western blotting were as follows: rabbit antibodies to CD63 (EXOAB-CD63A-1) and CD81 (EXOAB-CD81-1, System Biosciences, Palo Alto, CA, USA); mouse antibodies to γ-actin (FUJIFILM Wako Pure Chemical) and albumin (sc-270165, Santa Cruz Biotech, Santa Cruz, CA, USA); HRP-linked secondary goat antibody to rabbit IgG (EXOAB-HRP, System Biosciences) and sheep antibody to mouse IgG (NA931, GE Healthcare, Chicago, IL, USA).

Isolation and culture of rat vascular SMCs

Primary rat aortic smooth muscle cells (RASM) were isolated from a thoracic aorta of normal Wistar rats with an enzyme digestion method by modifying the previously published protocol [19]. Wistar rats (5-week-old) were deeply anesthetized with urethane (1.5 g/kg, i.p.) and euthanized by exsanguination. The thoracic aorta was isolated under sterile conditions. After removal of fat, the aorta was dissected into rings (1–2 mm) in an ice-cold Hank's balanced Salt Solution (−) (FUJIFILM Wako Pure Chemical). To remove endothelium and adventitia, the rings were reacted with an M199 medium containing 3.5 mg/ml collagenase (FUJIFILM Wako Pure Chemical) (37°C, 15 min). After pipetting, the rings were digested with an M199 medium containing 3.5 mg/ml collagenase again (37°C, 30 min). Then, the rings were minced by pipetting and centrifuged (200 × g, 5 min, 4°C). The supernatant was discarded, and the pellet was resuspended in 2.5 g/l trypsin/1 mM EDTA solution (Nacalai Tesque) diluted 2 times by TBS. After incubation (37°C, 30 min) and dispersion by pipetting, they were collected in a new tube and treated with a trypsin neutralizer solution (Thermo Fisher Scientific, Waltham, MA, USA). The supernatant was discarded after centrifugation (200 × g, 5 min, 4°C), and the cells were resuspended in Dulbecco's Modified Eagle's Medium (DMEM, FUJIFILM Wako Pure Chemical) supplemented with 20% fetal bovine serum (FBS). The resuspended cells were seed in a 35 mm-culture dish and passaged at

confluent. They (passage 4–10) were cultured in DMEM supplemented with 10% FBS and used for the following experiments.

Cell migration analysis by a boyden chamber assay

We examined the migration of RASM by a boyden chamber assay [36, 43]. Briefly, the polycarbonate membranes with an 8 μm pore size (Costar, Cambridge, MA, USA) were coated by 2% gelatin (FUJIFILM Wako Pure Chemical) in ddH$_2$O (37°C, 30 min). RASM (5.0×10^4 cells/well) were seeded in the upper chamber and treated for 48 hr with WsEV, SsEV (0.1, 0.3, 1.0 × 10^8 particles/m*l*) or PBS (Cont). After the treatment, they were fixed with 100% methanol (RT, 15 min) and stained with a Giemsa stain solution (Nacalai Tesque) diluted 15 times by ddH$_2$O (RT, 20 min). Non-migrated cells in the upper side of the polycarbonate membrane were wiped with a cotton swab. The migrated cells in the lower side were photographed and randomly counted on the basis of those of nuclei in three fields (×100) by using a light microscope (CKX31, Olympus Corp., Tokyo, Japan) equipped with a CCD camera (True Chrome II Plus, TUCSEN, Fujian, China).

Cell proliferation analysis by a bromodeoxyuridine (BrdU) incorporation assay

We examined the proliferation of RASM with a BrdU incorporation assay kit (Exalpha Biologicals, Shirley, MA, USA) as described previously [36, 43]. Briefly, RASM (4.0×10^3 cells/well) were seeded on a 96-well culture plate and treated for 48 hr with WsEV, SsEV (0.1, 0.3, 1.0 × 10^8 particles/m*l*) or PBS (Cont). The BrdU reagent was added to the wells for 36 hr in the presence of sEV or PBS. After the treatment, the cells were fixed with a fixing solution (RT, 30 min) and washed with the wash buffer three times. Then, they were treated with an anti-BrdU antibody (RT, 1 hr) and incubated with an HRP-conjugated anti-mouse IgG (1:2,000 dilution, RT, 30 min). Tetra-methyl benzidine (TMB) peroxidase substrate was added (RT, 30 min) followed by the addition of the stop solution. The differences between absorbance at 450 nm and 560 nm in the media were determined by using a microplate reader (Tristar3 LB941, Berthold Technologies, Bad Wildbad, Germany).

Uptake of sEV labeled with PKH67

To assess the uptake of plasma sEV into RASM, they were treated with WsEV or SsEV, which were labeled with PKH67 green fluorescence dye (Sigma Aldrich). WsEV or SsEV were reacted with PKH67 (4 μM, RT, 3 min), which was stopped with the same volume of sterilized PBS containing 10% bovine serum albumin (Nacalai Tesque). To wash the excess dye, the sEV-PKH67 solution was taken into a tube containing a sterilized 0.971 M sucrose solution in the bottom and ultracentrifuged (164,071 × g, 4°C, 35 min). The supernatants were removed by pipetting and the pellets were resuspended in sterilized PBS. RASM were treated for 2 hr with PKH67-labeled sEV (1.0×10^8 particles/m*l*) or PKH67-reacted PBS (Cont) and fixed with 4% paraformaldehyde (FUJIFILM Wako Pure Chemical) (4°C, 10 min). Nuclei were stained with 4', 6-diamidino-2-phenylindole (DAPI, Dojindo Laboratories, Kumamoto, Japan) (RT, 10 min) and photographed by using a fluorescence microscope (BX-51) with a digital camera (DP74) and CellSens standard dimension ver. 1.18 software (Olympus). Fluorescence density in a single cell was measured using an ImageJ software (National Institutes of Health, Bethesda, MD, USA).

Statistical analysis

Data are shown as means ± standard error of mean (SEM). Statistical analyses were performed using one-way ANOVA followed by Bonferroni's test for multiple comparisons and by Student's *t*-test between two groups. Values of *P*<0.05 were considered statistically significant.

RESULTS

Concentration and size distribution of plasma sEV from WKY and SHR

We first verified whether the vesicles isolated from plasma of WKY and SHR by the precipitation with polyethylene-glycol and ultracentrifugation exhibit the expected size profiles of sEV as previously reported [40]. The isolated vesicles from plasma of WKY and SHR distributed within the expected ranges with a diameter of 100–150 nm as determined by the tunable resistive pulse sensing analyses (Fig. 1a, b, n=3). These results suggest the successful plasma sEV isolation from WKY and SHR. Next, we compared the concentration and size between plasma sEV from WKY (WsEV) and SHR (SsEV). There was no significant difference in total concentration (Fig. 1c, n=3, 1.31 ± 0.07 × 10^{10} particles/m*l* in WsEV, 1.29 ± 0.31 × 10^{10} particles/m*l* in SsEV), mean diameter (Fig. 1d, n=3, 152.0 ± 8.0 nm in WsEV, 147 ± 5.4 nm in SsEV) or percentage of particles with a diameter of smaller than 150 nm (Fig. 1e, n=3, 67.7 ± 6.3% in WsEV, 73.7 ± 4.6% in SsEV) between WsEV and SsEV.

The protein expression of markers for sEV (CD63 and CD81), large EV (γ-actin) or plasma (albumin) in WsEV and SsEV

The protein expression of sEV markers (CD63 and CD81) [40] in WsEV and SsEV was examined by Western blotting. There was no difference in the expression of CD63 between WsEV and SsEV (Fig. 2a, n=3), while the expression of CD81 in SsEV was significantly lower than that in WsEV (Fig. 2b, n=3, *P*<0.05). The removal of other types of EVs and contaminating proteins was also examined. In WsEV or SsEV, the protein expression of large EV marker (γ-actin) and the plasma contaminants (albumin) were significantly lower than those in the positive control (Fig. 2c, n=3, *P*<0.01 vs. Large EV; Fig. 2d, n=3, *P*<0.01 vs. Plasma).

Effects of WsEV and SsEV on migration and proliferation in vascular SMCs

Next, we examined the effects of WsEV and SsEV on the cellular functions in RASM. WsEV (0.3, 1.0 × 10^8 particles/m*l*, 48 hr)
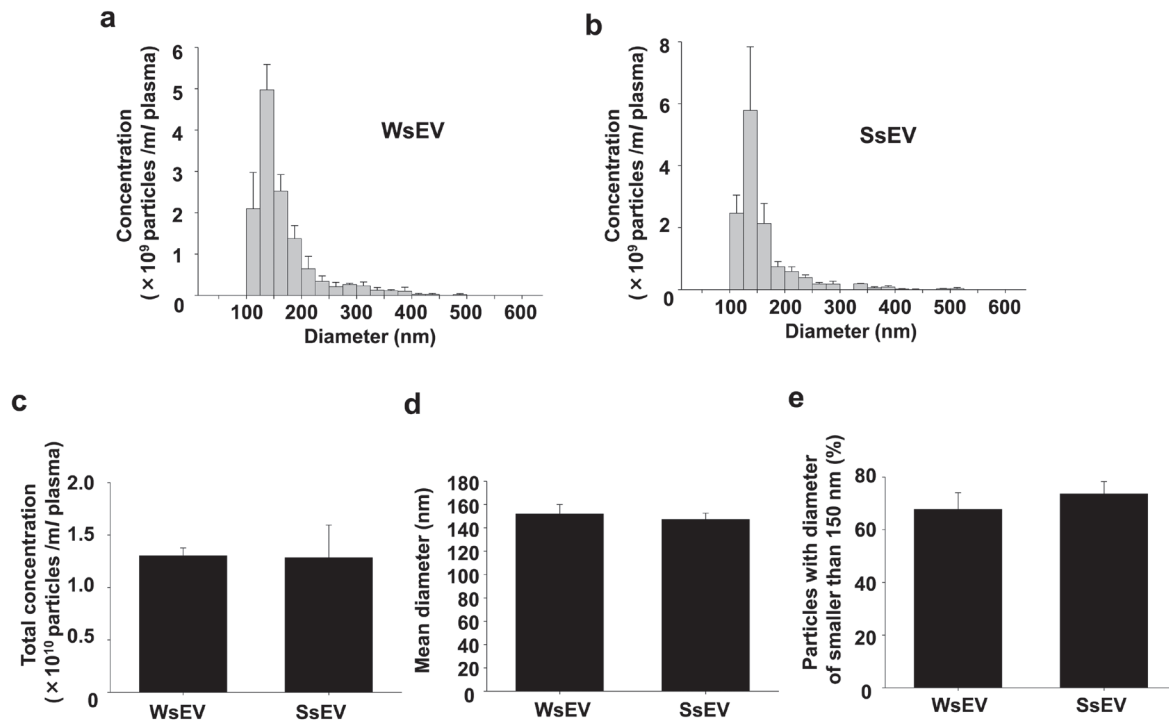
Fig. 1. Concentration and size distribution of small extracellular vesicles (sEV) in plasma of Wistar Kyoto rats (WKY) and spontaneously hypertensive rats (SHR). sEV were isolated from heparin (1 U/m*l*)-anticoagulated plasma in male WKY (6-week-old) and SHR (6-week-old) by precipitation with polyethylene-glycol and ultracentrifugation. Concentration and size distribution of the isolated sEV were measured by a tunable resistive pulse sensing analysis method using a qNANO instrument. (a, b) Concentration and size distribution of plasma sEV of WKY (WsEV, a) and SHR (SsEV, b) were shown. (c) Total concentration of WsEV and SsEV was shown (particles/m*l*). (d) Mean diameter of WsEV and SsEV was shown. (e) The percentage of particles with a diameter of smaller than 150 nm in total particles of WsEV and SsEV was shown. Results were expressed as means ± standard error of the mean in bar graphs (n=3).

and SsEV (1.0×10^8 particles/m*l*, 48 hr) significantly increased the migration in RASM (Fig. 3a, n=3, 0.3×10^8 particles/m*l* WsEV and 1.0×10^8 particles/m*l* SsEV, $P<0.05$ vs. Cont; 1.0×10^8 particles/m*l* WsEV, $P<0.01$ vs. Cont). Furthermore, WsEV (1.0×10^8 particles/m*l*, 48 hr) and SsEV (1.0×10^8 particles/m*l*, 48 hr) significantly increased the proliferation in RASM (Fig. 3b, n=6, $P<0.01$ vs. Cont). There was no difference in the migratory and proliferative effects between WsEV and SsEV.

Uptake of sEV into cells

The sEV mediate cellular function via internalization by phagocytosis, pinocytosis, or membrane fusion [24, 30, 44]. To examine the internalization of sEV, RASM were treated with WsEV or SsEV which were labeled with PKH67 green fluorescence dye. Both WsEV and SsEV (1.0×10^8 particles/m*l*, 2 hr) were taken into RASM. There was no significant difference in the amounts of uptake between WsEV and SsEV (Fig. 4, n=3).

DISCUSSION

The major findings of the present study are as follows: 1) There was no significant difference in the concentration and size distribution between WsEV and SsEV, while the protein expression of CD81 differed. 2) Both WsEV and SsEV were internalized into RASM, and then stimulated the migration and proliferation with a similar potency.

In the present study, the concentration of plasma sEV isolated from WKY and SHR was approximately 1.0–1.5×10^{10} particles/m*l* (Fig. 1). No other groups so far have reported the concentration of plasma sEV from WKY and SHR, while the concentration of plasma sEV in Sprague-Dawley [22, 35, 37, 46], Wistar [6], and Fisher 344 [9] rats was reported to be ranging between 10^8–10^{12} particles/m*l*. Therefore, the concentration of our sEV would be within the reasonable ranges and also was enough for the following analyses. In the present study, RASM were treated with sEV at 1.0×10^7–10^8 particles/m*l* (Figs. 3, 4). Other studies examined the effects of EV on cultured cells at wide-ranging concentrations between 10^5–10^9 particles/m*l* [5, 12, 50]. Then, there was no obvious deviation in the concentrations of sEV used between ours and others'.

A variety of proteins, such as tetraspanin (CD9, CD63, and CD81), major histocompatibility complex, and integrin, are expressed on the surface of sEV [39, 45]. In the present study, the protein expression of CD81 in SsEV was lower than WsEV (Fig. 2). It is assumed that the differences in the origins of SsEV and WsEV exist, since the expression profiles of surface proteins on sEV are different dependent on the EV-secreting cell types [24, 35]. Moreover, the surface proteins could potentially affect the
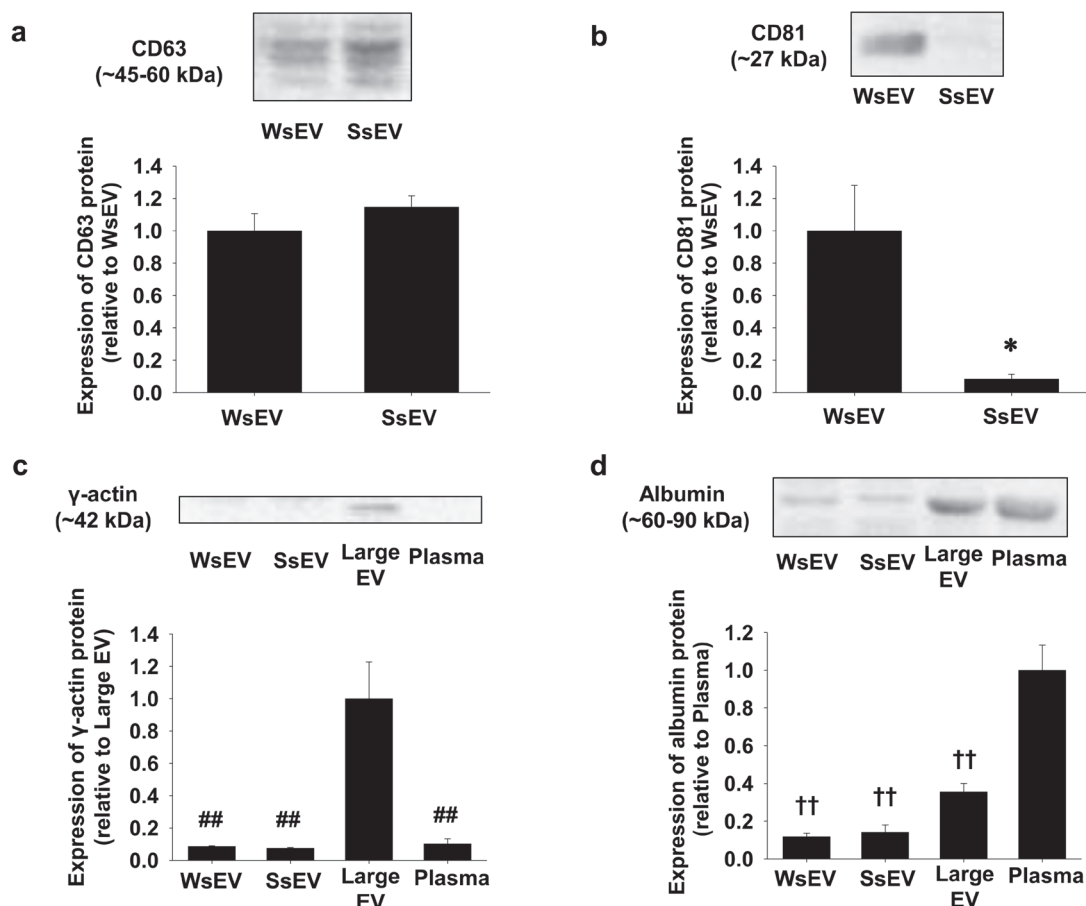
Fig. 2. The expression of marker proteins for small extracellular vesicles (sEV) (CD63 and CD81), large EV (γ-actin) or plasma (albumin) in plasma sEV of Wistar Kyoto rats (WKY) (WsEV) and spontaneously hypertensive rats (SHR) (SsEV). Total protein was extracted from WsEV and SsEV using radio-immunoprecipitation assay buffer. Expression of marker proteins in plasma sEV was examined by Western blotting using an antibody to CD63, CD81, γ-actin or albumin. The large EV isolated from plasma of normal male Wistar rats (8-week-old) by centrifugation (10,000 × g, 10 min, 4°C) and the plasma of Wistar rats (8-week-old) were loaded as positive control. Data were shown as fold increase relative to the expression level in WsEV (CD63 and CD81), large EV (γ-actin) or plasma (albumin). Results were expressed as means ± standard error of the mean in bar graphs (n=3). *$P<0.05$ vs. WsEV, ##$P<0.01$ vs. Large EV, ††$P<0.01$ vs. Plasma.

amounts of internalized sEV into the cell. For example, a degradation of surface protein on sEV by proteinase K can suppress the uptake of sEV in human ovarian cancer cells [15]. In addition, the anti-CD9 or -CD81 antibody prevents the HIV-1 entry into human T-lymphoblastoid reinforced by sEV [34]. In the present study, however, there was no significant difference in the amounts of uptake between WsEV and SsEV (Fig. 4). Therefore, CD81 would have no crucial role in the uptake of sEV. In addition, CD81 mediates antigen presentation [2], and the upregulation of CD81 induced by oxidative stress in endothelial cells was reported to promote the monocyte adhesion [31]. Although the increased concentration of sEV and the associated upregulation of CD81 in plasma of type II diabetes model rats were reported [14], downregulation of CD81 in sEV under pathological condition has not been reported to the best of our knowledge. Then the meanings of the decreased CD81 expression in SsEV remain to be clarified, which needs to be extensively explored in the future study.

Both WsEV and SsEV similarly stimulated the migration and proliferation of RASM in the present study (Fig. 3). The sEV derived from fetal bovine serum (FBS) and plasma of Sprague-Dawley rats were also reported to stimulate cell migration [33, 37]. These results suggest that the circulating sEV can activate cell migration or/and proliferation irrespective of their origins and that the observed effects of WsEV and SsEV on RASM are physiological but not pathological ones. We have recently reported that SsEV can mediate the increase of systolic blood pressure in WKY, while WsEV can mediate the decrease of systolic blood pressure in SHR [28]. Then, it is suggested that WsEV and SsEV would regulate the blood pressure via the actions on other tissues than vascular SMCs, including central nervous system, heart, kidney, and vascular endothelium, which potentially contribute to regulate the development of systemic hypertension [8, 23, 29, 32].

In summary, we, for the first time, demonstrated that plasma sEV in WKY and SHR are similarly uptaken into the cells and stimulate the migration and proliferation. Further researches are required to elucidate the underlying mechanisms of plasma sEV regulating pathology of systemic hypertension.
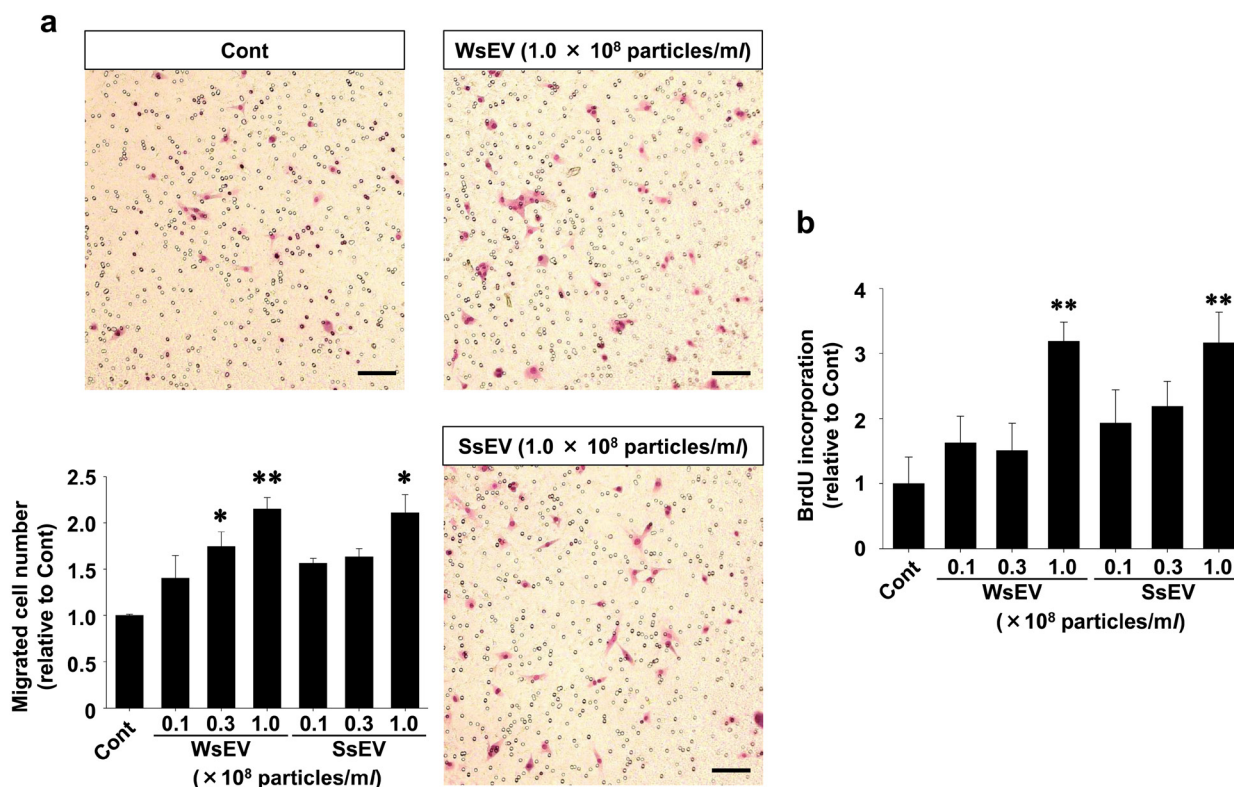
Fig. 3. Effects of small extracellular vesicles (sEV) in plasma of Wistar Kyoto rats (WKY) (WsEV) and spontaneously hypertensive rats (SHR) (SsEV) on migration and proliferation in vascular smooth muscle cells. (a) Migration of primary rat aortic smooth muscle cells (RASM) was determined by a boyden chamber assay. RASM were treated for 48 hr with WsEV, SsEV (0.1, 0.3 or 1.0 × 10⁸ particles/m*l*) or PBS (Cont). We observed the migrated RASM which were stained with Giemsa using a phase-contrast microscope. Data were shown as fold increase relative to the migrated cell number in Cont. Results were expressed as means ± standard error of the mean (SEM) (n=3) in bar graph. Scale bar: 100 μm. *$P<0.05$, **$P<0.01$ vs. Cont. (b) Proliferation of RASM was determined by a bromodeoxyuridine (BrdU) incorporation assay. RASM were stimulated for 48 hr with WsEV, SsEV (0.1, 0.3 or 1.0 × 10⁸ particles/m*l*) or PBS (Cont). In the presence of sEV or PBS, RASM were treated with BrdU for 36 hr. Incorporation of BrdU was measured by an immunostaining with anti-BrdU antibody. Data were shown as fold increase relative to Cont. Results were expressed as means ± SEM (n=6) in bar graph. **$P<0.01$ vs. Cont.
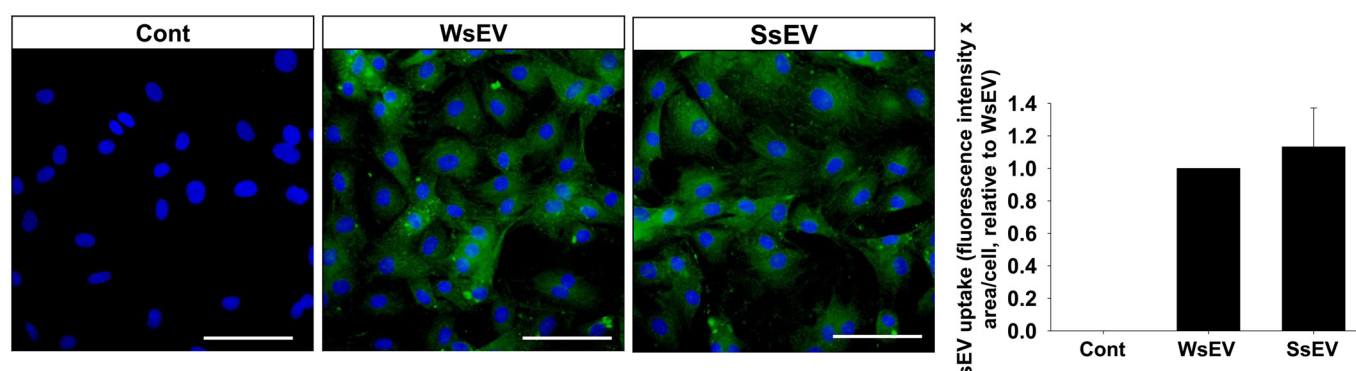

Fig. 4. Uptake of small extracellular vesicles (sEV) into cells. Primary rat aortic smooth muscle cells (RASM) were treated with plasma sEV of Wistar Kyoto rats (WKY) (WsEV) and spontaneously hypertensive rats (SHR) (SsEV) (1.0 × 10⁸ particles/m*l*, 2 hr) which were labeled with PKH67 green fluorescence dye (4 μM). For negative control (Cont), RASM were treated with vehicle (PBS) reacted with PKH67 by the same procedure as WsEV and SsEV. After the cells were fixed with 4% paraformaldehyde, the nuclei were stained with 4', 6-diamidino-2-phenylindole (DAPI), which were observed by a fluorescence microscope. The green fluorescence density (intensity × area) in the cells relative to WsEV was shown as means ± standard error of the mean (n=3) in bar graph. Green: PKH67; Blue: DAPI. Scale bar: 100 μm.

REFERENCES

1. Aliotta, J. M., Pereira, M., Wen, S., Dooner, M. S., Del Tatto, M., Papa, E., Goldberg, L. R., Baird, G. L., Ventetuolo, C. E., Quesenberry, P. J. and Klinger, J. R. 2016. Exosomes induce and reverse monocrotaline-induced pulmonary hypertension in mice. *Cardiovasc. Res.* **110**: 319–330. [Medline] [CrossRef]

2. Andreu, Z. and Yáñez-Mó, M. 2014. Tetraspanins in extracellular vesicle formation and function. *Front. Immunol.* **5**: 442. [Medline] [CrossRef]

3. Azmi, A. S., Bao, B. and Sarkar, F. H. 2013. Exosomes in cancer development, metastasis, and drug resistance: a comprehensive review. *Cancer Metastasis Rev.* **32**: 623–642. [Medline] [CrossRef]

4. Bang, C. and Thum, T. 2012. Exosomes: new players in cell-cell communication. *Int. J. Biochem. Cell Biol.* **44**: 2060–2064. [Medline] [CrossRef]

5. Bao, H., Chen, Y. X., Huang, K., Zhuang, F., Bao, M., Han, Y., Chen, X. H., Shi, Q., Yao, Q. P. and Qi, Y. X. 2018. Platelet-derived microparticles promote endothelial cell proliferation in hypertension via miR-142-3p. *FASEB J.* **32**: 3912–3923. [Medline] [CrossRef]

6. Baranyai, T., Herczeg, K., Onódi, Z., Voszka, I., Módos, K., Marton, N., Nagy, G., Mäger, I., Wood, M. J., El Andaloussi, S., Pálinkás, Z., Kumar, V., Nagy, P., Kittel, Á., Buzás, E. I., Ferdinandy, P. and Giricz, Z. 2015. Isolation of exosomes from blood plasma: Qualitative and quantitative comparison of ultracentrifugation and size exclusion chromatography methods. *PLoS One* **10**: e0145686. [Medline] [CrossRef]

7. Barile, L., Lionetti, V., Cervio, E., Matteucci, M., Gherghiceanu, M., Popescu, L. M., Torre, T., Siclari, F., Moccetti, T. and Vassalli, G. 2014. Extracellular vesicles from human cardiac progenitor cells inhibit cardiomyocyte apoptosis and improve cardiac function after myocardial infarction. *Cardiovasc. Res.* **103**: 530–541. [Medline] [CrossRef]

8. Basting, T. and Lazartigues, E. 2017. DOCA-salt hypertension: an update. *Curr. Hypertens. Rep.* **19**: 32. [Medline] [CrossRef]

9. Beninson, L. A., Brown, P. N., Loughridge, A. B., Saludes, J. P., Maslanik, T., Hills, A. K., Woodworth, T., Craig, W., Yin, H. and Fleshner, M. 2014. Acute stressor exposure modifies plasma exosome-associated heat shock protein 72 (Hsp72) and microRNA (miR-142-5p and miR-203). *PLoS One* **9**: e108748. [Medline] [CrossRef]

10. Brown, I. A. M., Diederich, L., Good, M. E., DeLalio, L. J., Murphy, S. A., Cortese-Krott, M. M., Hall, J. L., Le, T. H. and Isakson, B. E. 2018. Vascular smooth muscle remodeling in conductive and resistance arteries in hypertension. *Arterioscler. Thromb. Vasc. Biol.* **38**: 1969–1985. [Medline] [CrossRef]

11. Candelario, K. M. and Steindler, D. A. 2014. The role of extracellular vesicles in the progression of neurodegenerative disease and cancer. *Trends Mol. Med.* **20**: 368–374. [Medline] [CrossRef]

12. Chatterjee, V., Yang, X., Ma, Y., Cha, B., Meegan, J. E., Wu, M. and Yuan, S. Y. 2019. Endothelial microvesicles carrying Src-rich cargo impair adherens junction integrity and cytoskeleton homeostasis. *Cardiovasc. Res.* **7**: e46808. [Medline]

13. Choi, D. S., Kim, D. K., Kim, Y. K. and Gho, Y. S. 2013. Proteomics, transcriptomics and lipidomics of exosomes and ectosomes. *Proteomics* **13**: 1554–1571. [Medline] [CrossRef]

14. Davidson, S. M., Riquelme, J. A., Takov, K., Vicencio, J. M., Boi-Doku, C., Khoo, V., Doreth, C., Radenkovic, D., Lavandero, S. and Yellon, D. M. 2018. Cardioprotection mediated by exosomes is impaired in the setting of type II diabetes but can be rescued by the use of non-diabetic exosomes *in vitro*. *J. Cell. Mol. Med.* **22**: 141–151. [Medline] [CrossRef]

15. Escrevente, C., Keller, S., Altevogt, P. and Costa, J. 2011. Interaction and uptake of exosomes by ovarian cancer cells. *BMC Cancer* **11**: 108. [Medline] [CrossRef]

16. Gangoda, L., Boukouris, S., Liem, M., Kalra, H. and Mathivanan, S. 2015. Extracellular vesicles including exosomes are mediators of signal transduction: are they protective or pathogenic? *Proteomics* **15**: 260–271. [Medline] [CrossRef]

17. Howitt, J. and Hill, A. F. 2016. Exosomes in the pathology of neurodegenerative diseases. *J. Biol. Chem.* **291**: 26589–26597. [Medline] [CrossRef]

18. Jalali, S., Ramanathan, G. K., Parthasarathy, P. T., Aljubran, S., Galam, L., Yunus, A., Garcia, S., Cox, R. R. Jr., Lockey, R. F. and Kolliputi, N. 2012. Mir-206 regulates pulmonary artery smooth muscle cell proliferation and differentiation. *PLoS One* **7**: e46808. [Medline] [CrossRef]

19. Kwartler, C., Zhou, P., Kuang, S.Q., Duan, X.Y., Gong, L. and Milewicz, D. 2016. Vascular smooth muscle cell isolation and culture from mouse aorta. *Bio Protoc.* **6**: e2045. [CrossRef]

20. Lai, R. C., Arslan, F., Lee, M. M., Sze, N. S. K., Choo, A., Chen, T. S., Salto-Tellez, M., Timmers, L., Lee, C. N., El Oakley, R. M., Pasterkamp, G., de Kleijn, D. P. V. and Lim, S. K. 2010. Exosome secreted by MSC reduces myocardial ischemia/reperfusion injury. *Stem Cell Res. (Amst.)* **4**: 214–222. [Medline] [CrossRef]

21. Liu, X., Yuan, W., Yang, L., Li, J. and Cai, J. 2019. miRNA profiling of exosomes from spontaneous hypertensive rats using next-generation sequencing. *J. Cardiovasc. Transl. Res.* **12**: 75–83. [Medline] [CrossRef]

22. Minghua, W., Zhijian, G., Chahua, H., Qiang, L., Minxuan, X., Luqiao, W., Weifang, Z., Peng, L., Biming, Z., Lingling, Y., Zhenzhen, W., Jianqing, X., Huihui, B., Xiaozhong, W. and Xiaoshu, C. 2018. Plasma exosomes induced by remote ischaemic preconditioning attenuate myocardial ischaemia/reperfusion injury by transferring miR-24. *Cell Death Dis.* **9**: 320. [Medline] [CrossRef]

23. Mordi, I., Mordi, N., Delles, C. and Tzemos, N. 2016. Endothelial dysfunction in human essential hypertension. *J. Hypertens.* **34**: 1464–1472. [Medline] [CrossRef]

24. Mulcahy, L. A., Pink, R. C. and Carter, D. R. F. 2014. Routes and mechanisms of extracellular vesicle uptake. *J. Extracell. Vesicles* **3**: 1–14. [Medline] [CrossRef]

25. Nguyen, M. A., Karunakaran, D., Geoffrion, M., Cheng, H. S., Tandoc, K., Perisic Matic, L., Hedin, U., Maegdefessel, L., Fish, J. E. and Rayner, K. J. 2018. Extracellular vesicles secreted by atherogenic macrophages transfer microrna to inhibit cell migration. *Arterioscler. Thromb. Vasc. Biol.* **38**: 49–63. [Medline] [CrossRef]

26. Niu, C., Wang, X., Zhao, M., Cai, T., Liu, P., Li, J., Willard, B., Zu, L., Zhou, E., Li, Y., Pan, B., Yang, F. and Zheng, L. 2016. Macrophage foam cell-derived extracellular vesicles promote vascular smooth muscle cell migration and adhesion. *J. Am. Heart Assoc.* **5**: e004099. [Medline] [CrossRef]

27. Otani, K., Fujioka, Y., Okada, M. and Yamawaki, H. 2019. Optimal isolation method of small extracellular vesicles from rat plasma. *Int. J. Mol. Sci.* **20**: 4780. [Medline] [CrossRef]

28. Otani, K., Yokoya, M., Kodama, T., Hori, K., Matsumoto, K., Okada, M. and Yamawaki, H. 2018. Plasma exosomes regulate systemic blood pressure in rats. *Biochem. Biophys. Res. Commun.* **503**: 776–783. [Medline] [CrossRef]

29. Phillips, M. I. and Sumners, C. 1998. Angiotensin II in central nervous system physiology. *Regul. Pept.* **78**: 1–11. [Medline] [CrossRef]

30. Raposo, G. and Stoorvogel, W. 2013. Extracellular vesicles: exosomes, microvesicles, and friends. *J. Cell Biol.* **200**: 373–383. [Medline] [CrossRef]

31. Rohlena, J., Volger, O. L., van Buul, J. D., Hekking, L. H. P., van Gils, J. M., Bonta, P. I., Fontijn, R. D., Post, J. A., Hordijk, P. L. and Horrevoets, A. J. G. 2009. Endothelial CD81 is a marker of early human atherosclerotic plaques and facilitates monocyte adhesion. *Cardiovasc. Res.* **81**: 187–196. [Medline] [CrossRef]

32. Seravalle, G. and Grassi, G. 2017. Obesity and hypertension. *Pharmacol. Res.* **122**: 1–7. [Medline] [CrossRef]

33. Shelke, G. V., Lässer, C., Gho, Y. S. and Lötvall, J. 2014. Importance of exosome depletion protocols to eliminate functional and RNA-containing

extracellular vesicles from fetal bovine serum. *J. Extracell. Vesicles* **3**: 1–8. [Medline] [CrossRef]

34. Sims, B., Farrow, A. L., Williams, S. D., Bansal, A., Krendelchtchikov, A. and Matthews, Q. L. 2018. Tetraspanin blockage reduces exosome-mediated HIV-1 entry. *Arch. Virol.* **163**: 1683–1689. [Medline] [CrossRef]

35. Sosanya, N. M., Kumar, R., Clifford, J. L., Chavez, R., Dimitrov, G., Srinivasan, S., Gautam, A., Trevino, A. V., Williams, M., Hammamieh, R., Cheppudira, B. P., Christy, R. J. and Crimmins, S. L. 2019. Identifying plasma derived extracellular vesicle (EV) contained biomarkers in the development of chronic neuropathic pain. *J. Pain* S1526-5900(18)30775-2. [Medline]

36. Sugiyama, A., Hirano, Y., Okada, M. and Yamawaki, H. 2018. Endostatin stimulates proliferation and migration of myofibroblasts isolated from myocardial infarction model rats. *Int. J. Mol. Sci.* **19**: E741. [Medline] [CrossRef]

37. Takov, K., Yellon, D. M. and Davidson, S. M. 2018. Comparison of small extracellular vesicles isolated from plasma by ultracentrifugation or size-exclusion chromatography: yield, purity and functional potential. *J. Extracell. Vesicles* **8**: 1560809. [Medline] [CrossRef]

38. Tan, L., Wu, H., Liu, Y., Zhao, M., Li, D. and Lu, Q. 2016. Recent advances of exosomes in immune modulation and autoimmune diseases. *Autoimmunity* **49**: 357–365. [Medline] [CrossRef]

39. Théry, C., Ostrowski, M. and Segura, E. 2009. Membrane vesicles as conveyors of immune responses. *Nat. Rev. Immunol.* **9**: 581–593. [Medline] [CrossRef]

40. Théry, C., Witwer, K. W., Aikawa, E., Alcaraz, M. J., Anderson, J. D., Andriantsitohaina, R., Antoniou, A., Arab, T., Archer, F., Atkin-Smith, G. K., Ayre, D. C., Bach, J. M., Bachurski, D., Baharvand, H., Balaj, L., Baldacchino, S., Bauer, N. N., Baxter, A. A., Bebawy, M., Beckham, C., Bedina Zavec, A., Benmoussa, A., Berardi, A. C., Bergese, P., Bielska, E., Blenkiron, C., Bobis-Wozowicz, S., Boilard, E., Boireau, W., Bongiovanni, A., Borràs, F. E., Bosch, S., Boulanger, C. M., Breakefield, X., Breglio, A. M., Brennan, M. Á., Brigstock, D. R., Brisson, A., Broekman, M. L. D., Bromberg, J. F., Bryl-Górecka, P., Buch, S., Buck, A. H., Burger, D., Busatto, S., Buschmann, D., Bussolati, B., Buzás, E. I., Byrd, J. B., Camussi, G., Carter, D. R. F., Caruso, S., Chamley, L. W., Chang, Y. T., Chen, C., Chen, S., Cheng, L., Chin, A. R., Clayton, A., Clerici, S. P., Cocks, A., Cocucci, E., Coffey, R. J., Cordeiro-da-Silva, A., Couch, Y., Coumans, F. A., Coyle, B., Crescitelli, R., Criado, M. F., D'Souza-Schorey, C., Das, S., Datta Chaudhuri, A., de Candia, P., De Santana, E. F., De Wever, O., Del Portillo, H. A., Demaret, T., Deville, S., Devitt, A., Dhondt, B., Di Vizio, D., Dieterich, L. C., Dolo, V., Dominguez Rubio, A. P., Dominici, M., Dourado, M. R., Driedonks, T. A. P., Duarte, F. V., Duncan, H. M., Eichenberger, R. M., Ekström, K., El Andaloussi, S., Elie-Caille, C., Erdbrügger, U., Falcón-Pérez, J. M., Fatima, F., Fish, J. E., Flores-Bellver, M., Försönits, A., Frelet-Barrand, A., Fricke, F., Fuhrmann, G., Gabrielsson, S., Gámez-Valero, A., Gardiner, C., Gärtner, K., Gaudin, R., Gho, Y. S., Giebel, B., Gilbert, C., Gimona, M., Giusti, I., Goberdhan, D. C., Görgens, A., Gorski, S. M., Greening, D. W., Gross, J. C., Gualerzi, A., Gupta, G. N., Gustafson, D., Handberg, A., Haraszti, R. A., Harrison, P., Hegyesi, H., Hendrix, A., Hill, A. F., Hochberg, F. H., Hoffmann, K. F., Holder, B., Holthofer, H., Hosseinkhani, B., Hu, G., Huang, Y., Huber, V., Hunt, S., Ibrahim, A. G., Ikezu, T., Inal, J. M., Isin, M., Ivanova, A., Jackson, H. K., Jacobsen, S., Jay, S. M., Jayachandran, M., Jenster, G., Jiang, L., Johnson, S. M., Jones, J. C., Jong, A., Jovanovic-Talisman, T., Jung, S., Kalluri, R., Kano, S. I., Kaur, S., Kawamura, Y., Keller, E. T., Khamari, D., Khomyakova, E., Khvorova, A., Kierulf, P., Kim, K. P., Kislinger, T., Klingeborn, M., Klinke, D. J. 2nd., Kornek, M., Kosanović, M. M., Kovács, Á. F., Krämer-Albers, E. M., Krasemann, S., Krause, M., Kurochkin, I. V., Kusuma, G. D., Kuypers, S., Laitinen, S., Langevin, S. M., Languino, L. R., Lannigan, J., Lässer, C., Laurent, L. C., Lavieu, G., Lázaro-Ibáñez, E., Le Lay, S., Lee, M. S., Lee, Y. X. F., Lemos, D. S., Lenassi, M., Leszczynska, A., Li, I. T., Liao, K., Libregts, S. F., Ligeti, E., Lim, R., Lim, S. K., Linē, A., Linnemannstöns, K., Llorente, A., Lombard, C. A., Lorenowicz, M. J., Lörincz, Á. M., Lötvall, J., Lovett, J., Lowry, M. C., Loyer, X., Lu, Q., Lukomska, B., Lunavat, T. R., Maas, S. L., Malhi, H., Marcilla, A., Mariani, J., Mariscal, J., Martens-Uzunova, E. S., Martin-Jaular, L., Martinez, M. C., Martins, V. R., Mathieu, M., Mathivanan, S., Maugeri, M., McGinnis, L. K., McVey, M. J., Meckes, D. G. Jr., Meehan, K. L., Mertens, I., Minciacchi, V. R., Möller, A., Møller Jørgensen, M., Morales-Kastresana, A., Morhayim, J., Mullier, F., Muraca, M., Musante, L., Mussack, V., Muth, D. C., Myburgh, K. H., Najrana, T., Nawaz, M., Nazarenko, I., Nejsum, P., Neri, C., Neri, T., Nieuwland, R., Nimrichter, L., Nolan, J. P., Nolte-'t Hoen, E. N., Noren Hooten, N., O'Driscoll, L., O'Grady, T., O'Loghlen, A., Ochiya, T., Olivier, M., Ortiz, A., Ortiz, L. A., Osteikoetxea, X., Østergaard, O., Ostrowski, M., Park, J., Pegtel, D. M., Peinado, H., Perut, F., Pfaffl, M. W., Phinney, D. G., Pieters, B. C., Pink, R. C., Pisetsky, D. S., Pogge von Strandmann, E., Polakovicova, I., Poon, I. K., Powell, B. H., Prada, I., Pulliam, L., Quesenberry, P., Radeghieri, A., Raffai, R. L., Raimondo, S., Rak, J., Ramirez, M. I., Raposo, G., Rayyan, M. S., Regev-Rudzki, N., Ricklefs, F. L., Robbins, P. D., Roberts, D. D., Rodrigues, S. C., Rohde, E., Rome, S., Rouschop, K. M., Rughetti, A., Russell, A. E., Saá, P., Sahoo, S., Salas-Huenuleo, E., Sánchez, C., Saugstad, J. A., Saul, M. J., Schiffelers, R. M., Schneider, R., Schøyen, T. H., Scott, A., Shahaj, E., Sharma, S., Shatnyeva, O., Shekari, F., Shelke, G. V., Shetty, A. K., Shiba, K., Siljander, P. R., Silva, A. M., Skowronek, A., Snyder, O. L. 2nd., Soares, R. P., Sódar, B. W., Soekmadji, C., Sotillo, J., Stahl, P. D., Stoorvogel, W., Stott, S. L., *et al.* 2018. Minimal information for studies of extracellular vesicles 2018 (MISEV2018): a position statement of the International Society for Extracellular Vesicles and update of the MISEV2014 guidelines. *J. Extracell. Vesicles* **7**: 1535750. [Medline] [CrossRef]

41. Tong, Y., Ye, C., Ren, X. S., Qiu, Y., Zang, Y. H., Xiong, X. Q., Wang, J. J., Chen, Q., Li, Y. H., Kang, Y. M. and Zhu, G. Q. 2018. Exosome-mediated transfer of ACE (angiotensin-converting enzyme) from adventitial fibroblasts of spontaneously hypertensive rats promotes vascular smooth muscle cell migration. *Hypertension* **72**: 881–888. [Medline] [CrossRef]

42. Touyz, R. M., Alves-Lopes, R., Rios, F. J., Camargo, L. L., Anagnostopoulou, A., Arner, A. and Montezano, A. C. 2018. Vascular smooth muscle contraction in hypertension. *Cardiovasc. Res.* **114**: 529–539. [Medline] [CrossRef]

43. Usui, T., Sakatsume, T., Nijima, R., Otani, K., Kazama, K., Morita, T., Kameshima, S., Okada, M. and Yamawaki, H. 2014. Death-associated protein kinase 3 mediates vascular structural remodelling via stimulating smooth muscle cell proliferation and migration. *Clin. Sci.* **127**: 539–548. [Medline] [CrossRef]

44. Valadi, H., Ekström, K., Bossios, A., Sjöstrand, M., Lee, J. J. and Lötvall, J. O. 2007. Exosome-mediated transfer of mRNAs and microRNAs is a novel mechanism of genetic exchange between cells. *Nat. Cell Biol.* **9**: 654–659. [Medline] [CrossRef]

45. van Niel, G., D'Angelo, G. and Raposo, G. 2018. Shedding light on the cell biology of extracellular vesicles. *Nat. Rev. Mol. Cell Biol.* **19**: 213–228. [Medline] [CrossRef]

46. Vicencio, J. M., Yellon, D. M., Sivaraman, V., Das, D., Boi-Doku, C., Arjun, S., Zheng, Y., Riquelme, J. A., Kearney, J., Sharma, V., Multhoff, G., Hall, A. R. and Davidson, S. M. 2015. Plasma exosomes protect the myocardium from ischemia-reperfusion injury. *J. Am. Coll. Cardiol.* **65**: 1525–1536. [Medline] [CrossRef]

47. Weidle, U. H., Birzele, F., Kollmorgen, G. and Rüger, R. 2017. The multiple roles of exosomes in metastasis. *Cancer Genomics Proteomics* **14**: 1–15. [Medline] [CrossRef]

48. Xie, Z., Wang, X., Liu, X., Du, H., Sun, C., Shao, X., Tian, J., Gu, X., Wang, H., Tian, J. and Yu, B. 2018. Adipose-derived exosomes exert proatherogenic effects by regulating macrophage foam cell formation and polarization. *J. Am. Heart Assoc.* **7**: e007442. [Medline] [CrossRef]

49. Zhao, L., Luo, H., Li, X., Li, T., He, J., Qi, Q., Liu, Y. and Yu, Z. 2017. Exosomes derived from human pulmonary artery endothelial cells shift the balance between proliferation and apoptosis of smooth muscle cells. *Cardiology* **137**: 43–53. [Medline] [CrossRef]

50. Zhu, L., Xiao, R., Zhang, X., Lang, Y., Liu, F., Yu, Z., Zhang, J., Su, Y., Lu, Y., Wang, T., Luo, S., Wang, J., Liu, M. L., Dupuis, J., Jing, Z. C., Li, T., Xiong, W. and Hu, Q. 2019. Spermine on endothelial extracellular vesicles mediates smoking-induced pulmonary hypertension partially through calcium-sensing receptor. *Arterioscler. Thromb. Vasc. Biol.* **39**: 482–495. [Medline] [CrossRef]